

## ■ Flow Chemistry

# A Visible-Light-Powered Polymerization Method for the Immobilization of Enantioselective Organocatalysts into Microreactors

Rico Warias,<sup>[a]</sup> Daniele Ragno,<sup>[b]</sup> Alessandro Massi,<sup>[b]</sup> and Detlev Belder\*<sup>[a]</sup>

**Abstract:** A versatile one-step photopolymerization approach for the immobilization of enantioselective organocatalysts is presented. Chiral organocatalyst-containing monoliths based on polystyrene divinylbenzene copolymer were generated inside channels of microfluidic chips. Exemplary performance tests were performed for the monolithic Hayashi–Jørgensen catalyst in continuous flow, which showed good results for the Michael addition of aldehydes to nitroalkenes in terms of stereoselectivity and catalyst stability with minimal consumption of reagents and solvents.

Flow synthesis has gained much attention in recent years as a powerful alternative over conventional batch approaches due to superior process control, hazard reduction, and the avenue of exploring novel process windows.<sup>[1–5]</sup> Especially the use of continuous flow microreactors has become a popular means of quickly mapping synthetic parameters, and process intensification.<sup>[6–8]</sup> Using such miniaturized approaches can help to minimize reagent and catalyst consumption, as well as reducing waste production, with an overall higher reaction efficiency.<sup>[9,10]</sup> These benefits were already exploited in academia and industry for the production of fine chemicals and API (active pharmaceutical ingredient) precursors and flow chemistry itself has been seen as sustainable technology.<sup>[11–14]</sup> Further, the integration of heterogeneous catalysts inside micro-flow reactors provides another „green“ approach. Its benefits, like no demand for separation of the catalytic species from the resulting reaction mixture, a reduction of catalysts mechanical deg-


radation and deactivation (limited contact with air and moisture) and continuous production with catalyst TON increase, are often improving the system's overall productivity.<sup>[5,15–17]</sup>


Three main strategies for catalyst immobilization inside microreactors are described in the literature, namely the wall-coated, the packed bed, and the monolithic approach.<sup>[15,18]</sup> Despite the very good mass transfer and the minimal pressure drop, wall coated flow reactors lack in the loading of the desired catalyst, whereas packed bed reactors seem to be superior.<sup>[19]</sup> On the other hand, one drawback of using a particulate packed bed lies in the troublesome processes packing and anchoring the catalyst beads which are becoming more difficult within minimized reactor volumes. The implementation of monoliths into a micro-flow regime is a well-studied topic. Main advantages of these porous networks are their excellent mass-transfer properties, low pressure drop, and ease of preparation.<sup>[20–22]</sup>

A variety of porous materials have been investigated for this purpose,<sup>[23]</sup> such as inorganic materials,<sup>[24]</sup> metal–organic frameworks (MOFs),<sup>[25,26]</sup> and covalent–organic frameworks (COFs).<sup>[27]</sup> For the immobilization of organic catalysts, porous organic polymers (POPs) are preferred as support material. These materials are well studied and have been used for a variety of applications such as stationary phases in separation science<sup>[28,29]</sup> and as reagent supports in continuous flow synthesis.<sup>[30–34]</sup> Various polymerization processes and modification protocols have been reported.<sup>[35–38]</sup> For polystyrene-based monoliths, most common preparation methods involve radical-initiated (thermal or photochemical) copolymerization of monomers in the presence of porogens inside the reactor.<sup>[39–41]</sup> Photochemical strategies for catalyst immobilization profit from shorter reaction times mild temperatures which extends the range of possible monomers that can be used. When light transparent glass microreactors are used, a site-specific localization of the catalyst material can be achieved. This is appealing when microfluidic lab-on-a-chip devices with complex channel networks and integrated functionalities are used, such as micromixers,<sup>[42]</sup> further reaction units,<sup>[43]</sup> or even subsequent analytics.<sup>[44–46]</sup> Light transparent glass microreactors are also attractive for photochemical or photocatalytic reactions in micro-flow.<sup>[47–50]</sup> While thermally initiated polymerization is well established,<sup>[22,51,52]</sup> respective methods for photo-initiated polymerization of catalyst supports are rare. To the best of our knowledge, there is just a single example focusing on photo-initiated polymerization of an organic monolith with an application in organocatalysis.<sup>[53]</sup> There, a DMAP functionalized polystyrene-

[a] R. Warias, Prof. D. Belder  
Institute of Analytical Chemistry  
Leipzig University, Linnéstraße 3, 04103 Leipzig (Germany)  
E-mail: belder@uni-leipzig.de

[b] Dr. D. Ragno, Prof. A. Massi  
Department of Chemical and Pharmaceutical Sciences  
University of Ferrara, Via L. Borsari 46, 44121 Ferrara (Italy)

 Supporting information and the ORCID identification number(s) for the author(s) of this article can be found under:  
<https://doi.org/10.1002/chem.202002063>.

 © 2020 The Authors. Published by Wiley-VCH GmbH. This is an open access article under the terms of Creative Commons Attribution NonCommercial License, which permits use, distribution and reproduction in any medium, provided the original work is properly cited and is not used for commercial purposes.

based monolith was synthesized inside an Omnifit glass column (10.0×6.6 mm) through a photo-induced two-step protocol (fabrication of the monolith with an activated ester followed by catalyst displacement) and finally applied for acylation reactions.

Herein, we present a new method for the immobilization of enantioselective organocatalysts into microreactors using visible light-initiated polymerization. The formation of an organic monolith based on polystyrene is achieved straightforwardly without any need for further chemical modification steps. These new functionalized microreactors were tested in organocatalytic flow processes evaluating their chemical efficiency and stability over time.

The approach described here is based on previous work which focused on the fabrication of polystyrene monolithic microreactors functionalized with the Ley–Arvidsson–Yamamoto (S)-5-(pyrrolidin-2-yl)-1*H*-tetrazole organocatalyst<sup>[54]</sup> as well as on the TMS-protected Hayashi–Jørgensen (HJ) catalyst immobilized on silica and its application in chip devices with multiple functionalities.<sup>[55]</sup> For the latter approach, one challenge was the rather elaborate multi-step process for the creation of packed bed reactors inside microfluidic chips including the synthesis of the catalyst particles and the slurry packing process. Herein, a one-step photo-initiated immobilization strategy for the TMS-protected HJ catalyst on monolithic poly(styrene-*co*-divinylbenzene) is presented and its activity tested in enantioselective C–N- and C–C-bond forming flow reactions.

A starting point for the development of a photo-curable porous polymer-supported organocatalyst was the work of Levkin and co-workers who presented the first visible-light photopolymerization of a poly(styrene-*co*-divinylbenzene)-monolith,<sup>[56]</sup> as well as the work of Ismail et al. presenting its application on a microfluidic platform for radiochemistry studies.<sup>[57]</sup> Accordingly, first part of our study consisted in the synthesis of the HJ styrenyl derivative (Monomer-HJ, Figure 1A) through the Cu<sup>I</sup>-catalyzed azide-alkyne 1,3-dipolar cycloaddition (CuAAC) of a propargyl HJ derivative and 1-(azidomethyl)-4-vinylbenzene (see the Supporting Information for details). With the Monomer-HJ in our hands, we developed a suitable polymerization protocol. To this end, a solution was prepared containing photoinitiators (*S*-camphorquinone, CQ, 1.6 μmol; ethyl-*N*-dimethylbenzoate, EDAB, 6.7 μmol; *N*-methoxy-phenylpyridinium tetrafluoroborate, NMPPT, 6.9 μmol), monomers (Monomer-HJ, 0.019 mmol; styrene, STY, 0.121 mmol; divinylbenzene, DVB, 0.051 mmol), and porogens (1-decanol, 24 μL; 2-propanol, 20 μL) with residue solvent (acetonitrile, 10 μL) from the photoinitiator stock solution (Figure 1A, see Supporting Information for further details).

This resulting pre-polymer solution was vortexed, duly degassed by a gentle N<sub>2</sub> stream for 10 min, and finally sonicated for 20 min. The solution was transferred by pipetting it into the glass microreactor. For initial experiments, an in-house manufactured device with a straight channel design of the microreactor and adjacent packing channel was chosen (76×26×

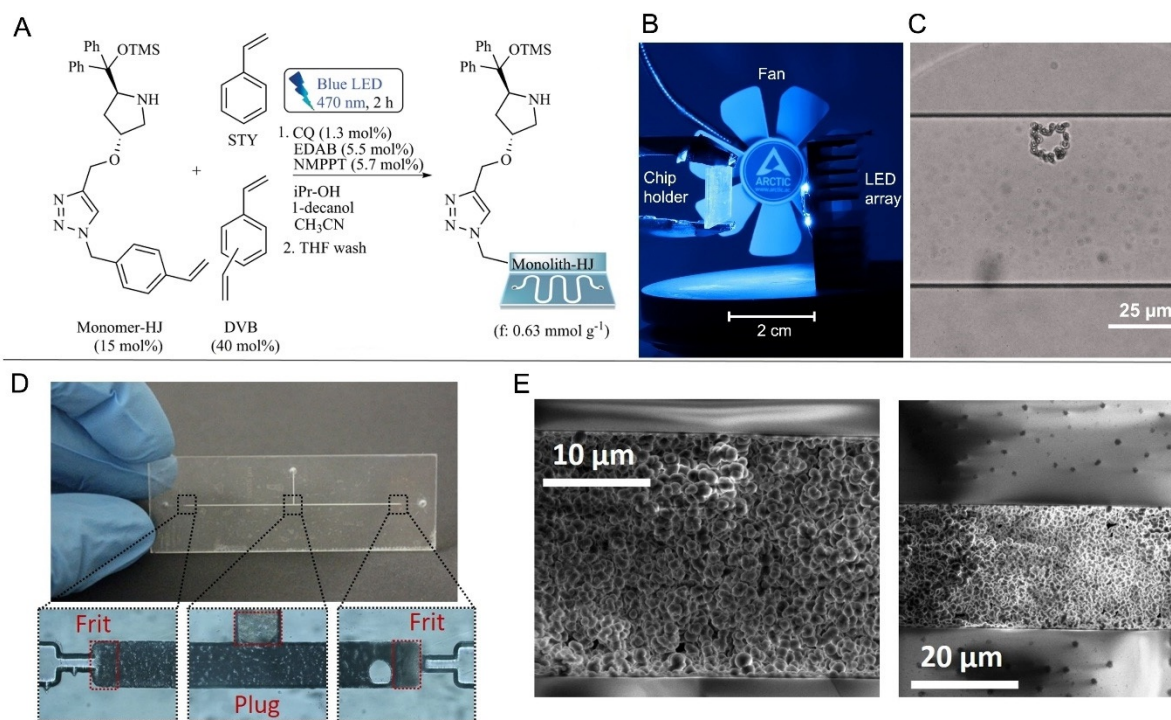


**Figure 1.** A) General reaction Scheme: pre-polymer mixture containing photoinitiators (*S*-camphorquinone (CQ, 1.6 μmol), ethyl-*N*-dimethylbenzoate (EDAB, 6.7 μmol)*N*-methoxy-phenyl-pyridinium tetrafluoroborate (NMPPT, 6.9 μmol)), monomers (monomer-HJ (0.019 mmol), styrene (STY, 0.121 mmol), divinylbenzene (DVB, 0.051 mmol)), and porogens (1-decanol (24 μL) 2-propanol (20 μL) in CH<sub>3</sub>CN (10 μL)). Irradiation with 470 nm LED source (2x LED array, 70 mm x 20 mm, 2x 126 lm) for 2 h, followed by THF flush (0.5 μL min<sup>-1</sup>) inside the chip for 2 h. B) Assembly for photopolymerization with LED array as used for microreactor preparation. C) Targeted photopolymerized structure by using an inverted epifluorescence microscope equipped with a 473 nm laser (Cobolt, Sweden). D) Photograph of the chip after polymerization procedure. Light microscopic pictures showing the retaining elements (porous acrylate-based polymers). E) SEM images of the chips cross section showing the monoliths macroporous structure.

2 mm in size, empty reactor volume ca. 300 nL). Once the chip was filled, the openings were sealed with adhesive tape and the microreactor was placed in front (2 cm distance) of a 470 nm LED source with similar size of the chip (2×LED array, 70 mm×20 mm, 2×126 lm). The polymerization could be followed visually by the increasing opaqueness. After 30 minutes, the polymerized material was recognizable. To assure a complete polymerization the chip was flipped every half an hour for a total illumination time of 2 hours. To prevent movement of the solution by thermal convection, the microreactor and LED array were cooled by a fan and temperature kept at 25–30 °C (Figure 1B). After the polymerization was completed, the microreactor was flushed with THF for approximately 2 hours to remove the monolith porogens and non-reacted monomers. During this process, <sup>1</sup>H-NMR measurements of the effluent assured for complete removal. The last step of the reactor preparation was closing the packing channel via targeted photopolymerization of acrylates.<sup>[54]</sup> In Figure 1D, a resulting microfluidic device can be seen with additional microscopic images of the microreactor channels. Scanning electron microscopy (SEM) measurements showed the characteristic monolithic structure with a pore size in the range of macropores (> 50 nm, Figure 1E).

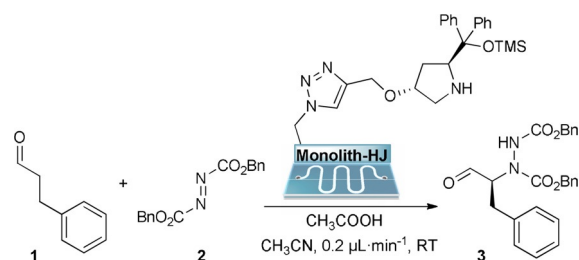
The comparison between two different microreactors confirmed the good reproducibility of the polymerization process, as shown in the SEM in Figure 1E (see Supporting Information for further details). In addition to the presented method for illuminating the entire chip, it is also possible to create polymer structures of smaller dimensions free of their positional selection through targeted laser irradiation (Figure 1C).

For the determination of catalyst loading of Monolith-HJ, the polymerization procedure was performed under batch conditions applying the same parameters as for the full-chip irradiation (details in Supporting Information). Elemental analysis of the resulting polymer particles revealed an average loading of 0.63 mmol g<sup>-1</sup>.

To investigate organocatalytic flow reactions and results on the catalytic performance of Monolith-HJ, the chip was integrated inside an on-line HPLC/MS system (detailed description in the Supporting Information). This allowed the transfer of little portions of the reactors effluent for an on-line analysis in real-time.

Initially, the flow-through behavior of the fabricated device was evaluated using the asymmetric  $\alpha$ -amination of aliphatic aldehyde **1** with dibenzyl azodicarboxylate (DBAD) **2** as the benchmark (Scheme 1). This model reaction was performed under the conditions previously employed with the silica-supported counterpart for a direct comparison.<sup>[55]</sup> This on-line HPLC/MS analysis revealed the formation of adduct **3** with a much higher enantiomeric excess (50% vs. 6% ee). Furthermore, the low pressure drop of just 1 bar at the applied flow rate of 0.2  $\mu\text{L min}^{-1}$  allows operating the setup with economic low pressure pumps.

After this explorative study, the catalytic efficiency of Monolith-HJ was further evaluated performing the Michael addition of aldehydes on activated alkenes as a more efficient transformation for the TMS-protected HJ catalyst.<sup>[58,59]</sup> Hence, the reac-



**Scheme 1.** Asymmetric  $\alpha$ -amination reaction. Reaction mixture: **1** (6.25 mmol L<sup>-1</sup>), **2** (1.25 mmol L<sup>-1</sup>) and CH<sub>3</sub>COOH (0.62 mmol L<sup>-1</sup>) as co-catalyst in pure CH<sub>3</sub>CN.

tion mixture consisting of an aliphatic aldehyde **4** (0.3 mmol L<sup>-1</sup>), a nitro-styrene derivative **5** (0.03 mmol L<sup>-1</sup>) and benzoic acid (0.013 mmol L<sup>-1</sup>) in acetonitrile was pumped through the catalytic microreactor with a flow rate of 0.1  $\mu\text{L min}^{-1}$  (Table 1). The addition products **6** were obtained with excellent diastereomeric and enantiomeric ratios, thus proving the effectiveness of the approach.

In our initial experiments, homemade glass chips were used. To prove this technology being widely applicable, we extend our study to commercially available microfluidic glass chips. For this purpose, a microreactor chip (Micronit) with an internal volume of about 18  $\mu\text{L}$  was used (photograph in Figure 2A). We were able to straightforwardly transfer the procedure described above. By omitting the polymeric retaining elements, the microreactors preparation protocol was simplified significantly (see the Supporting Information).

**Table 1.** Evaluation of catalyst performance under continuous flow conditions.<sup>[a]</sup>

Entry	R <sup>1</sup>	R <sup>2</sup>	Product	d.r. <sup>[b]</sup>	e.r. <sup>[c]</sup>
1	Me	Ph	<b>6a</b>	83:17	83:17
2	Et	Ph	<b>6b</b>	84:16	89:11
3	Me	4-ClC <sub>6</sub> H <sub>4</sub>	<b>6c</b>	91:9	90:10
4	Et	4-ClC <sub>6</sub> H <sub>4</sub>	<b>6d</b>	89:11	90:10
5	Me	4-MeC <sub>6</sub> H <sub>4</sub>	<b>6e</b>	85:15	94:6
6	Et	4-MeC <sub>6</sub> H <sub>4</sub>	<b>6f</b>	90:10	95:5

[a] Conditions: aldehyde **4** (0.30 mmol L<sup>-1</sup>), nitro-styrene **5** (0.03 mmol L<sup>-1</sup>), PhCOOH (0.013 mmol L<sup>-1</sup>) in pure CH<sub>3</sub>CN. Flow rate of 0.1  $\mu\text{L min}^{-1}$ , room temperature and a residence time of about 10 min (detailed description in the Supporting Information). For on-line analysis, 2  $\mu\text{L}$  of the reactors effluent were injected onto the HPLC-MS setup using a two-position switching valve. [b] d.r. was determined by integration of the corresponding peak areas of the extracted ion chromatogram (EIC) of the product from sampling after a run time of approx. 2 h. [c] e.r. was determined by HPLC on chiral stationary phase. HPLC: Chiralpak IG-3, 250 mm, 4.6 mm i.d. Mobile phase: 1 mL min<sup>-1</sup>, CH<sub>3</sub>CN/H<sub>2</sub>O (60/40 vol% with 0.1 mM sodium formate).

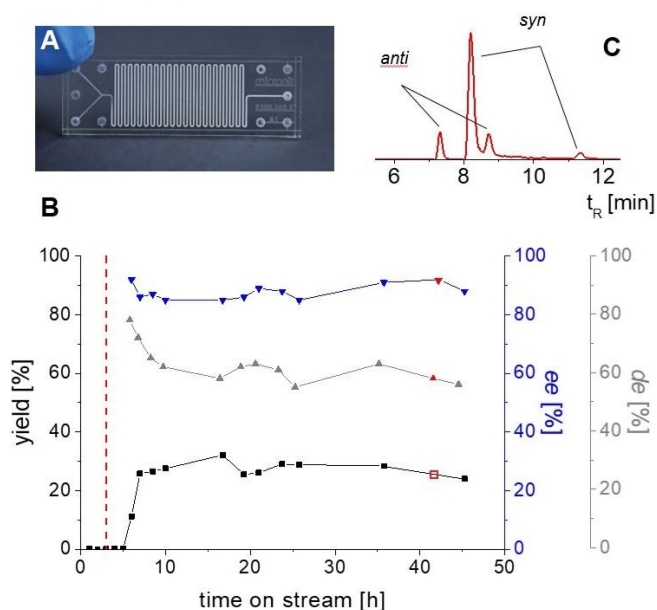


**Figure 2.** A) Photograph of the commercial glass microreactor (R300.500.2, Micronit GmbH, Germany). B) Yield of the model reaction as a function of the reactor run time. In red (dashed), first detection of non-reacted **5**. The reaction mixture (same substrates of Table 1, entry 6) consisted of **4** ( $0.3 \text{ mmol L}^{-1}$ ) and **5** ( $0.03 \text{ mmol L}^{-1}$ ) with benzoic acid ( $0.013 \text{ mmol L}^{-1}$ ) in  $\text{CH}_3\text{CN}$ . An applied flow rate of  $0.1 \mu\text{L min}^{-1}$  (1 bar) resulted in a residence time of about 90 min. The flow reaction was performed at room temperature. *de* was determined by integration of the corresponding peak areas of the extracted ion chromatogram (EIC) of the product. *ee* was determined as *de* after HPLC on chiral stationary phase. HPLC: Chiralpak IG-3, 50 mm, 4.6 mm i.d. Mobile phase:  $0.4 \text{ mL min}^{-1}$ ,  $\text{CH}_3\text{CN}/\text{H}_2\text{O}$  (60/40 vol% with  $0.1 \text{ mM}$  sodium formate). C) Red curve: MS-chromatogram ( $m/z$  258) from on-line measurement at a run time of 42.25 h.

The catalytic performance of Monolith-HJ was tested within the commercial device using the Michael reaction leading to adduct **6f** (Table 1, entry 6). In addition to the information about catalyst diastereo- and enantioselectivity, a statement about catalyst stability over time should be made. Thus, a total volume of  $300 \mu\text{L}$  of reactant solution was pumped into the microreactor, allowing the reaction to be monitored over time up to 50 hours at a flow rate of  $0.1 \mu\text{L min}^{-1}$ . As shown in Figure 2B, a steady-state yield of about 25–30% for **6f** together with an average *de* of 60% and *ee* of 88% were maintained constant throughout this long-term stability experiment.

Furthermore, we found out that complete removal of the monolithic material could be achieved by heating the chip at  $550^\circ\text{C}$  for over 24 hours without affecting the integrity of the channels (slow heating and cooling procedure required, more details in the Supporting Information). Possible residues could also be removed by flushing the chip with piranha solution. Overall, by this protocol microreactors could be restored and used again. This is especially appealing for method development in academic research.

In summary, we have presented a novel method for the immobilization of the Hayashi–Jørgensen catalyst inside glass chip-microreactors. This catalyst was incorporated by visible-light photoinduced polymerization inside a polystyrene monolith with macroporous structure. Continuous flow Michael addi-

tion of aldehydes to nitroalkenes was successfully performed observing good values of stereocontrol and catalyst stability over time.

We believe that the disclosed immobilization procedure applies to a variety of monomers functionalized with different organocatalysts. With this as well as with the microreactors recovery the rapid evaluation of catalyst performance is possible enabling a screening of reaction conditions for a target process with reduced waste of time and reagents. Optimization of monolith porosity, immobilization of different organic species as well as the integration of additional on-chip functionalities will be the object of forthcoming investigations.

## Acknowledgements

Funded by the Deutsche Forschungsgemeinschaft (DFG, German Research Foundation), Project number BE 1922/12-2, In-Chem. Open access funding enabled and organized by Projekt DEAL.

## Conflict of interest

The authors declare no conflict of interest.

**Keywords:** flow chemistry · immobilization · microreactors · organocatalysis · photopolymerization

- [1] R. L. Hartman, J. P. McMullen, K. F. Jensen, *Angew. Chem. Int. Ed.* **2011**, *50*, 7502–7519; *Angew. Chem.* **2011**, *123*, 7642–7661.
- [2] J. Wegner, S. Ceylan, A. Kirschning, *Adv. Synth. Catal.* **2012**, *354*, 17–57.
- [3] I. R. Baxendale, *J. Chem. Technol. Biotechnol.* **2013**, *88*, 519–552.
- [4] A. Adamo, R. L. Beingessner, M. Behnam, J. Chen, T. F. Jamison, K. F. Jensen, J.-C. M. Monbaliu, A. S. Myerson, E. M. Revalor, D. R. Snead, et al., *Science* **2016**, *352*, 61–67.
- [5] M. B. Plutschack, B. Pieber, K. Gilmore, P. H. Seeberger, *Chem. Rev.* **2017**, *117*, 11796–11893.
- [6] K. Geyer, J. D. C. Codée, P. H. Seeberger, *Chem. Eur. J.* **2006**, *12*, 8434–8442.
- [7] T. Noël, V. Hessel, in *Microreactors Prep. Chem.* (Ed.: W. Reschetilowski), Wiley-VCH Verlag GmbH & Co. KGaA, **2013**, pp. 273–295.
- [8] R. Porta, M. Benaglia, F. Coccia, S. Rossi, A. Puglisi, *Symmetry* **2015**, *7*, 1395–1409.
- [9] J. Wegner, S. Ceylan, A. Kirschning, *Chem. Commun.* **2011**, *47*, 4583–4592.
- [10] D. Barrow, S. Taylor, A. Morgan, L. Giles, in *Microreactors Org. Chem. Catal.* (Ed.: T. Wirth), Wiley-VCH Verlag GmbH & Co. KGaA, **2013**, pp. 1–33.
- [11] B. Gutmann, D. Cantillo, C. O. Kappe, *Angew. Chem. Int. Ed.* **2015**, *54*, 6688–6728; *Angew. Chem.* **2015**, *127*, 6788–6832.
- [12] R. Porta, M. Benaglia, A. Puglisi, *Org. Process Res. Dev.* **2016**, *20*, 2–25.
- [13] D. Dallinger, C. O. Kappe, *Curr. Opin. Green Sustain. Chem.* **2017**, *7*, 6–12.
- [14] S. B. Ötvös, M. A. Pericàs, C. O. Kappe, *Chem. Sci.* **2019**, *10*, 11141–11146.
- [15] R. Munirathinam, J. Huskens, W. Verboom, *Adv. Synth. Catal.* **2015**, *357*, 1093–1123.
- [16] I. Atodiresi, C. Vila, M. Rueping, *ACS Catal.* **2015**, *5*, 1972–1985.
- [17] A. Tanimu, S. Jaenicke, K. Alhooshani, *Chem. Eng. J.* **2017**, *327*, 792–821.
- [18] K. Masuda, T. Ichitsuka, N. Koumura, K. Sato, S. Kobayashi, *Tetrahedron* **2018**, *74*, 1705–1730.
- [19] M. Colella, C. Carlucci, R. Luisi, *Top. Curr. Chem.* **2018**, *376*, 46.

- [20] M. Mayr, B. Mayr, M. R. Buchmeiser, *Angew. Chem. Int. Ed.* **2001**, *40*, 3839–3842; *Angew. Chem.* **2001**, *113*, 3957–3960.
- [21] E. B. Anderson, M. R. Buchmeiser, *ChemCatChem* **2012**, *4*, 30–44.
- [22] R. Knob, V. Sahore, M. Sonker, A. T. Woolley, *Biomicrofluidics* **2016**, *10*, 032901.
- [23] J. Zhang, J. Chen, S. Peng, S. Peng, Z. Zhang, Y. Tong, P. W. Miller, X.-P. Yan, *Chem. Soc. Rev.* **2019**, *48*, 2566–2595.
- [24] Z. Walsh, B. Paull, M. Macka, *Anal. Chim. Acta* **2012**, *750*, 28–47.
- [25] H.-C. Zhou, J. R. Long, O. M. Yaghi, *Chem. Rev.* **2012**, *112*, 673–674.
- [26] H. Furukawa, K. E. Cordova, M. O’Keeffe, O. M. Yaghi, *Science* **2013**, *341*, 1230444.
- [27] U. Díaz, A. Corma, *Coord. Chem. Rev.* **2016**, *311*, 85–124.
- [28] F. Svec, Y. Lv, *Anal. Chem.* **2015**, *87*, 250–273.
- [29] X. Yuan, R. D. Oleschuk, *Anal. Chem.* **2018**, *90*, 283–301.
- [30] V. Chiroli, M. Benaglia, A. Puglisi, R. Porta, R. P. Jumde, A. Mandoli, *Green Chem.* **2014**, *16*, 2798–2806.
- [31] P. Llanes, S. Sayalero, C. Rodríguez-Esrich, M. A. Pericàs, *Green Chem.* **2016**, *18*, 3507–3512.
- [32] P. Llanes, C. Rodríguez-Esrich, S. Sayalero, M. A. Pericàs, *Org. Lett.* **2016**, *18*, 6292–6295.
- [33] J. M. Tobin, T. J. D. McCabe, A. W. Prentice, S. Holzer, G. O. Lloyd, M. J. Paterson, V. Arrighi, P. A. G. Cormack, F. Vilela, *ACS Catal.* **2017**, *7*, 4602–4612.
- [34] D. Ragno, G. Di Carmine, A. Brandolese, O. Bortolini, P. P. Giovannini, A. Massi, *ACS Catal.* **2017**, *7*, 6365–6375.
- [35] O. Bortolini, A. Cavazzini, P. Dambrosio, P. Giovannini, L. Caciolli, A. Massi, S. Pacifico, D. Ragno, *Green Chem.* **2013**, *15*, 2981–2992.
- [36] S. Martín, R. Porcar, E. Peris, M. I. Burguete, E. García-Verdugo, S. V. Luis, *Green Chem.* **2014**, *16*, 1639–1647.
- [37] K. J. Barlow, V. Bernabeu, X. Hao, T. C. Hughes, O. E. Hutt, A. Polyzos, K. A. Turner, G. Moad, *React. Funct. Polym.* **2015**, *96*, 89–96.
- [38] J. L. Dores-Sousa, A. Fernández-Pumarega, J. D. Vos, M. Lämmerhofer, G. Desmet, S. Eeltink, *J. Sep. Sci.* **2019**, *42*, 522–533.
- [39] F. Svec, *J. Chromatogr. A* **2010**, *1217*, 902–924.
- [40] K. Flook, Y. Agroskin, C. Pohl, *J. Sep. Sci.* **2011**, *34*, 2047–2053.
- [41] S. Eeltink, S. Wouters, J. L. Dores-Sousa, F. Svec, *J. Chromatogr. A* **2017**, *1498*, 8–21.
- [42] X. Liu, K. F. Jensen, *Green Chem.* **2013**, *15*, 1538–1541.
- [43] C.-C. Lee, G. Sui, A. Elizarov, C. J. Shu, Y.-S. Shin, A. N. Dooley, J. Huang, A. Daridon, P. Wyatt, D. Stout, et al., *Science* **2005**, *310*, 1793–1796.
- [44] S. Fritzsche, S. Ohla, P. Glaser, D. S. Giera, M. Sickert, C. Schneider, D. Belder, *Angew. Chem. Int. Ed.* **2011**, *50*, 9467–9470; *Angew. Chem.* **2011**, *123*, 9639–9642.
- [45] K. M. Krone, R. Warias, C. Ritter, A. Li, C. G. Acevedo-Rocha, M. T. Reetz, D. Belder, *J. Am. Chem. Soc.* **2016**, *138*, 2102–2105.
- [46] J. J. Heiland, R. Warias, C. Lotter, L. Mauritz, P. J. W. Fuchs, S. Ohla, K. Zeidler, D. Belder, *Lab. Chip* **2017**, *17*, 76–81.
- [47] S. Das, V. Chandra Srivastava, *Photochem. Photobiol. Sci.* **2016**, *15*, 714–730.
- [48] D. C. Fabry, E. Sugiono, M. Rueping, *React. Chem. Eng.* **2016**, *1*, 129–133.
- [49] Y. Matsushita, T. Ichimura, N. Ohba, S. Kumada, K. Sakeda, T. Suzuki, H. Tanibata, T. Murata, *Pure Appl. Chem.* **2007**, *79*, 1959–1968.
- [50] Y. Matsushita, N. Ohba, S. Kumada, K. Sakeda, T. Suzuki, T. Ichimura, *Chem. Eng. J.* **2008**, *135*, S303–S308.
- [51] M. Baumann, I. R. Baxendale, S. V. Ley, N. Nikbin, C. D. Smith, *Org. Biomol. Chem.* **2008**, *6*, 1587–1593.
- [52] K. A. Roper, M. B. Berry, S. V. Ley, *Beilstein J. Org. Chem.* **2013**, *9*, 1781–1790.
- [53] F. R. Bou-Hamdan, K. Krüger, K. Tauer, D. T. McQuade, P. H. Seeberger, *Aust. J. Chem.* **2013**, *66*, 213–217.
- [54] R. Greco, L. Caciolli, A. Zaghi, O. Pandoli, O. Bortolini, A. Cavazzini, C. D. Risi, A. Massi, *React. Chem. Eng.* **2016**, *1*, 183–193.
- [55] R. Warias, A. Zaghi, J. J. Heiland, S. K. Piendl, K. Gilmore, P. H. Seeberger, A. Massi, D. Belder, *ChemCatChem* **2018**, *10*, 5382–5385.
- [56] Z. Walsh, P. A. Levkin, V. Jain, B. Paull, F. Svec, M. Macka, *J. Sep. Sci.* **2010**, *33*, 61–66.
- [57] R. Ismail, J. Irribaren, M. Rashed Javed, A. Machness, R. M. van Dam, P. Yun Keng, *RSC Adv.* **2014**, *4*, 25348–25356.
- [58] C. A. Wang, Z. K. Zhang, T. Yue, Y. L. Sun, L. Wang, W. D. Wang, Y. Zhang, C. Liu, W. Wang, *Chem. Eur. J.* **2012**, *18*, 6718–6723.
- [59] E. Alza, S. Sayalero, P. Kasaplar, D. Almaşi, M. A. Pericàs, *Chem. Eur. J.* **2011**, *17*, 11585–11595.

---

Manuscript received: April 27, 2020

Accepted manuscript online: May 26, 2020

Version of record online: September 17, 2020